



OPEN ACCESS

EDITED BY

Alex J. Poulton,
Heriot-Watt University,
United Kingdom

REVIEWED BY

Mitsuhide Sato,
Nagasaki University, Japan
Sven Alexander Kranz,
Florida State University, United States

*CORRESPONDENCE

Thomas J. Ryan-Keogh
tryankeogh@csir.co.za

SPECIALTY SECTION

This article was submitted to
Marine Biogeochemistry,
a section of the journal
Frontiers in Marine Science

RECEIVED 04 April 2022

ACCEPTED 16 September 2022

PUBLISHED 12 October 2022

CITATION

Singh A, Thomalla SJ, Fietz S and
Ryan-Keogh TJ (2022) Spatial and
temporal variability of phytoplankton
photophysiology in the Atlantic
Southern Ocean.
Front. Mar. Sci. 9:912856.
doi: 10.3389/fmars.2022.912856

COPYRIGHT

© 2022 Singh, Thomalla, Fietz and
Ryan-Keogh. This is an open-access
article distributed under the terms of
the [Creative Commons Attribution
License \(CC BY\)](https://creativecommons.org/licenses/by/4.0/). The use, distribution
or reproduction in other forums is
permitted, provided the original
author(s) and the copyright owner(s)
are credited and that the original
publication in this journal is cited, in
accordance with accepted academic
practice. No use, distribution or
reproduction is permitted which does
not comply with these terms.

Spatial and temporal variability of phytoplankton photophysiology in the Atlantic Southern Ocean

Asmita Singh^{1,2}, Sandy J. Thomalla¹, Susanne Fietz²
and Thomas J. Ryan-Keogh^{1*}

¹Southern Ocean Carbon-Climate Observatory (SOCCO), Smart Places, Council for Scientific and Industrial Research (CSIR), Cape Town, South Africa, ²Department of Earth Sciences, Stellenbosch University, Stellenbosch, South Africa

Active chlorophyll-a fluorescence was measured during five summer research cruises (2008 – 2016), spanning the Atlantic sector of the Southern Ocean. This unique data set provides information for assessing zonal, inter-annual and intra-seasonal variability (early versus late summer) of photosynthetic efficiency (F_v/F_m). The zonal variability of F_v/F_m showed a typical latitudinal decline from a maximum in the Polar Frontal Zone (PFZ) (0.24 ± 0.03) to a minimum in the Southern Antarctic Circumpolar Current Zone (SACCZ) (0.18 ± 0.07). The inter-annual variability in F_v/F_m (between each cruise) was the highest in the SACCZ, while the Antarctic Zone (AZ) exhibited low inter-annual variability. Intra-seasonal variability between the zones was limited to a significantly higher mean F_v/F_m in the PFZ and AZ in early summer compared to late summer. Intra-seasonal variability between the cruises was, however, inconsistent as higher mean F_v/F_m in early summer were seen during some years as opposed to others. Ancillary physical and biogeochemical parameters were also assessed to investigate potential direct and indirect drivers of co-variability with F_v/F_m through a series of statistical t-tests, where significant differences in F_v/F_m were used as focus points to interrogate the plausibility of co-variance. Inter-zonal variability of surface seawater temperature (SST) and Silicate:Phosphate (Si:P) ratios were highlighted as co-varying with F_v/F_m in all zones, whilst community structure played an indirect role in some instances. Similarly, inter-annual variability in F_v/F_m co-varied with SST, Nitrate:Phosphate (N:P) and Si:P ratios in the PFZ, AZ and SACCZ, while community structure influenced inter-annual variability in the PFZ and SACCZ. Intra-seasonal variability in F_v/F_m was linked to all the ancillary parameters, except community structure in the AZ, whilst different ancillary parameters dominated differences during each of the cruises. These results were further scrutinized with a Principal Component Analysis for a subset of co-located data points, where N:P and Si:P ratios emerged as the principal indirect drivers of F_v/F_m variability. This study highlights the scope for using F_v/F_m to reflect the net response of phytoplankton photophysiology to environmental adjustments and accentuates the complex interplay of different physical and biogeochemical parameters that act simultaneously and oftentimes

antagonistically, influencing inter-zonal, inter-annual and intra-seasonal variability of F_v/F_m .

KEYWORDS

Fast Induction and Relaxation (FIRe) fluorometry, fluorescence, physical and biogeochemical parameters, phytoplankton photophysiology, photosynthetic efficiency, zonal variability, inter-annual variability, intra-seasonal variability

1 Introduction

The Southern Ocean (SO) hosts a diverse, unique and complex ecosystem (Harris, 2006), which is vital to the global uptake, sequestration and export of carbon from the atmosphere to the ocean's interior through the biological carbon pump (BCP) (Arrigo et al., 2008; Nunn et al., 2013; DeVries and Weber, 2017). The functioning of the SO BCP assists in the regulation of global atmospheric carbon dioxide (CO_2) levels (Takahashi et al., 2002), and thus in the modulation of Earth's climate (Hauck et al., 2015). Phytoplankton are essential to the SO BCP and, therefore, an understanding of the temporal and spatial distribution of photophysiology and the drivers of variability is important (Petrou et al., 2016; Deppeler and Davidson, 2017). Measurements of photosynthetic efficiency (F_v/F_m) provide information on the effects of physiological stress on the photosynthetic apparatus of phytoplankton cells and hence, are indicative of the potential for primary production. Factors that directly and indirectly impact phytoplankton photophysiology and primary productivity include physical conditions (e.g., seawater temperature and solar irradiation; Arrigo et al., 2010; Heiden et al., 2019), ambient nutrients (e.g., Boyer et al., 2013), and community structure (e.g., Suggestt et al., 2009). These conditions vary regionally and under seasonal extremes in the SO, driving large fluctuations in phytoplankton physiology and primary production that impact the efficiency of the BCP (Moore et al., 2013; Deppeler and Davidson, 2017).

The frontal features of the Antarctic Circumpolar Current (ACC) define zones in the SO (Orsi et al., 1995; Pollard et al., 2002) that are distinguished by unique physical and chemical characteristics (Deppeler and Davidson, 2017), which in turn influence the spatial distribution of phytoplankton community structure, metabolic rates, F_v/F_m (Suggestt et al., 2009) and primary production (Boyer et al., 2013). For example, warmer surface seawater temperature (SST) with decreasing latitude directly impact phytoplankton metabolic rates (Marañón et al., 2018), which may indirectly impact photosynthetic responses. Although F_v/F_m is not directly related to adjustments in SST, relationships may arise as a secondary response that reflects an imbalance in cellular metabolism. The very cold SSTs of the high

latitude SO can also indirectly affect F_v/F_m by inducing changes in phytoplankton community structure (Feng et al., 2009; Finkel et al., 2010). Nutrient stress also directly impacts F_v/F_m (Spackeen et al., 2018) by curtailing photosynthesis when insufficient, resulting in lower F_v/F_m , and indirectly by impacting the temperature dependence of phytoplankton metabolic rates (Finkel et al., 2010; Marañón et al., 2018) and community structure. Concomitant with this is light availability, which also impacts nutrient demand (Sunda and Huntsman, 1995; Strzpek et al., 2012) further impacting F_v/F_m .

Since the seasonal cycle alters heat flux, water temperatures, stratification, mixed layer depth (MLD), nutrient supply and light availability, it is expected that there will be some seasonal influence on the variability of photophysiology, both directly and indirectly (Suggestt et al., 2006). Under low light conditions (i.e., in winter or when MLD's are deep in early spring), phytoplankton effectively maximise photosynthesis by increasing the size of their light-harvesting antenna or the number of photosynthetic units to increase light absorption (Sunda and Huntsman, 1997; Sunda and Huntsman, 2012; Strzpek et al., 2019). This photophysiological strategy to low light increases intracellular iron requirements, thereby decreasing F_v/F_m despite the availability of nutrients implied by deep MLD's (Boyd, 2002). In late spring and early summer, high F_v/F_m values have been observed in the Sub-Antarctic Zone (SAZ) (Ryan-Keogh et al., 2018), supposedly driven by a shoaling of the MLD's (or depths of active mixing), that provided the required light environment to support positive net community production and bloom formation (Mahadevan et al., 2012; Brody and Lozier, 2014), while nutrients were still plentiful from winter resupply (Tagliabue et al., 2014). On the contrary, in late summer and autumn, nutrient depletion from phytoplankton utilization has been proposed as the likely driver of low F_v/F_m (Ryan-Keogh et al., 2018). An important seasonal aspect that adds to the F_v/F_m variability is the occurrence of iron limitation, despite high macronutrient availability. High rates of biological activity in the SO are typically supported by high concentrations of the macronutrients nitrate and phosphate but are often seasonally constrained by low concentrations of the micronutrient iron (de Baar et al., 1990; Morel and Price, 2003), which likely causes a temporary lowering in F_v/F_m . Strong

seasonal variability is also typical of the Marginal Ice Zone (MIZ), where higher summer SST melts the sea ice (increasing micronutrient supply) and contributes to the formation of a shallow stratified freshwater lens that improves the light environment, which together yields higher F_v/F_m and increased rates of phytoplankton production (Arrigo et al., 2008; Demidov et al., 2012).

As temperature, light, and nutrients also affect community structure the above temporal and regional changes are expected to be indirectly reflected in F_v/F_m variability through a change in community structure. For example, when neither light nor nutrients are limiting, such as conditions occurring south of the Polar Front (PF) in early summer, diatoms thrive (Boyd et al., 2010), which typically display high values of F_v/F_m (Ryan-Keogh et al., 2017). Low concentrations of silicic acid toward the end of the phytoplankton growing season, drive a shift in community structure towards flagellates and haptophytes as diatom production is constrained (Hutchins et al., 2001; Boyd et al., 2010). These smaller celled phytoplankton tend to thrive in low nutrient conditions due to their high surface area to volume ratio advantage, and typically have a lower F_v/F_m than diatoms (Suggett et al., 2009). A strong seasonal succession is also evident in the MIZ where *P. antarctica* tends to dominate the MIZ (Sow et al., 2020), along with large contributions of diatoms (Arrigo et al., 1999), which should result in higher F_v/F_m . However, in the MIZ, phytoplankton metabolism is primarily impacted by low SSTs that result in an upper limit to growth and productivity (Strzepek et al., 2019), which may indirectly drive lower F_v/F_m .

The complex spatial and temporal interplay of factors controlling phytoplankton photophysiology, production rates and the BCP's efficiency are expected to vary with climate change (Matebr and Hirst, 1999; Le Quéré et al., 2010). Warming and freshening of the SO due to global climate change (e.g., Durack and Wijffels, 2010) will enhance the degree of stratification (Hutchins and Boyd, 2016; Sallée et al., 2021), while an intensification of the westerly winds will deepen the MLD in summer (Sallée et al., 2021). These projected conditions are expected to lead to significant alterations in F_v/F_m through changes in light and nutrient availability. In addition, adjustments in phytoplankton community structure and function are expected whereby species that can physiologically adapt to outcompete under future physical and chemical conditions would be favored (Deppeler and Davidson, 2017; Strzepek et al., 2019). Such changes in the phytoplankton community are likely to impact F_v/F_m making it a powerful tool for assessing the individual and cumulative response of phytoplankton to the multitude of expected environmental adjustments associated with climate change.

Despite numerous incubation studies in the Atlantic SO that have probed phytoplankton's photophysiological response to the manipulation of climatic stressors (e.g., Hutchins and Boyd, 2016; Ryan-Keogh et al., 2018; Viljoen et al., 2018), *in situ*

investigations of the photophysiological response of phytoplankton to environmental changes over time and across the polar ocean are sparse. This data gap highlights the need for multi-year *in situ* monitoring programs with broad spatial coverage that can bridge numerous space-time knowledge gaps associated with a changing climate. Active chlorophyll-a (Chl-a) fluorescence can serve such ambitious monitoring programmes, as it is a powerful tool for deriving F_v/F_m as a proxy for the response of phytoplankton to physical, chemical or biological stressors (Kolber and Falkowski, 1992; Kolber et al., 1998). F_v/F_m can provide high-resolution observations of *in situ* phytoplankton photophysiology and subsequent primary production, thus enhancing our ability to understand the sensitivity of phytoplankton's response to climate drivers. To our knowledge, this is the first multi-year austral summer study (5 cruises spanning 7 years) of *in situ* phytoplankton photophysiology that provides a unique opportunity for investigating the inter-zonal, inter-annual and intra-seasonal (early versus late summer) variability and distribution of F_v/F_m , alongside ancillary physical and biogeochemical parameters for the Atlantic SO.

2 Materials and methods

Photophysiological, environmental and biogeochemical data were collected from the ship's non-toxic underway scientific seawater supply (~7 m water depth) during five South African National Antarctic Expedition (SANAE) cruises on the RV SA Agulhas and the RV SA Agulhas II to the Atlantic SO. The cruises were: SANAE 48 (December 2008 – February 2009), SANAE 49 (December 2009 – February 2010), SANAE 53 (November 2013 – February 2014), SANAE 54 (December 2014 – February 2015) and SANAE 55 (December 2015 – February 2016); hereafter referred to as S48, S49, S53, S54 and S55, respectively. An ongoing focus of the SANAE voyages is the repeat occupation of the hydrographic GoodHope Line (GHL) between South Africa and Antarctica, which has traversed the extent of the ACC since 2004 (Swart et al., 2012). Only data collected between 10°W and 10°E on the GHL were retained for this analysis. All active Chl-a fluorescence measurements which passed the quality control (QC) procedures below are displayed in Figure 1, with the individual frontal positions for each cruise indicated. The southbound transect typically takes place in December while the northbound return transect typically occurs in February. The cruise start and end dates appear in Supplementary Table S1, along with the frontal positions of the south- and northbound transects per cruise.

Measurements of phytoplankton photophysiology from active Chl-a fluorescence were made continuously (every 30 - 90 seconds) and coupled with 4-hourly measurements of a suite of underway physical and biogeochemical parameters. The

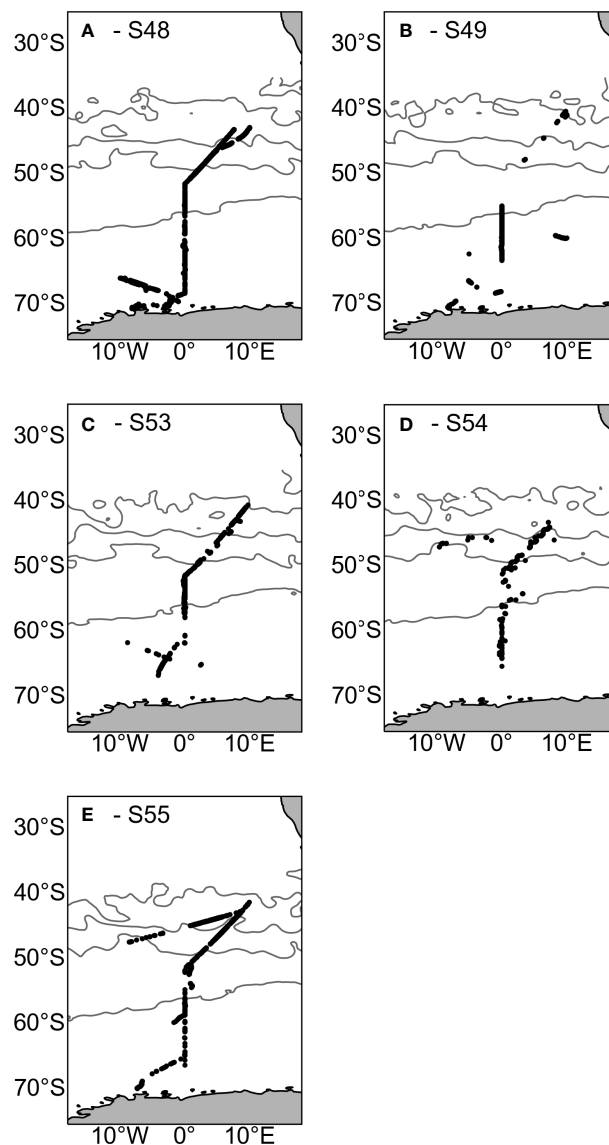


FIGURE 1

Individual plots of the night-time active chlorophyll-a fluorescence measurement points which passed the quality control (QC) procedure for each cruise independently (A) SANAE 48 (S48), (B) SANAE 49 (S49), (C) SANAE 53 (S53), (D) SANAE 54 (S54) and (E) SANAE 55 (S55), along with the respective frontal positions indicated for each cruise from north to south - Sub-Tropical Front (STF), Sub-Antarctic Front (SAF), Antarctic Polar Front (PF) and Southern Boundary (SBdy), delineating the corresponding zones between the fronts (Sub-Antarctic Zone (SAZ), Polar Frontal Zone (PFZ), Antarctic Zone (AZ) and Southern Antarctic Circumpolar Current Zone (SACCZ)).

geographical frontal positions for each month of every cruise were obtained from maps of absolute dynamic topography from the CLS/AVISO product (Rio et al., 2011) using the boundary definitions from Swart et al. (2012). The positions of the Sub-Tropical Front (STF), Sub-Antarctic Front (SAF), Antarctic Polar Front (PF) and Southern Boundary (SBdy) for each individual cruise can be found in Supplementary Table S1. These fronts form zones, as defined in Pollard et al. (2002), as the SAZ, the Polar Frontal Zone (PFZ), the Antarctic Zone (AZ), and the Southern Antarctic Circumpolar Current Zone

(SACCZ), respectively. Cruise-specific frontal positions were used to separate the zones for the statistical analyses in this paper, i.e., to compare zonal differences.

2.1 Active Chl-a fluorescence

Active Chl-a fluorescence data ($F_v = F_m - F_0$, where F_m is the maximum fluorescence and F_0 the initial fluorescence) were collected with a benchtop Fast Induction and Relaxation (FIRE)

system (Formerly Satlantic, now Seabird, S/N: 030) in underway flow-through mode (Gorbunov and Falkowski, 2004). The FIRE protocol consisted of 80 – 100 × 1 μs saturating flashlets with a 1 μs interval. Samples were continually replaced within a measurement interval of 30 - 90 seconds and 10 transients per measurement. To improve the signal-to-noise ratio, a pre-optimization transient averaging a 5-minute time window was applied across all cruises (Supplementary Table S2). Measurements were blank corrected on a daily basis using seawater filtered through a 0.2 μm filter (Cullen and Davis, 2003). Raw data were processed using the custom code Phytoplankton Photophysiology Utilities in Python 3.7 (Ryan-Keogh and Robinson, 2021) fitting the biophysical model of Kolber et al. (1998). The model fits the saturation phase of the data where the connectivity coefficient, ρ , was held at a constant value of 0.3 (Suggett et al., 2001) and the first flashlet was skipped (Ryan-Keogh and Robinson, 2021) to derive F_o , F_m and F_v/F_m .

2.1.1 Quality control

A series of quality control (QC) tests were implemented on the active Chl-a fluorescence data (Supplementary Table S2). (1) Measured values greater or less than the mean ± the standard deviation (SD), for each 5-minute averaged measurement, were excluded as outliers. (2) Data that fell outside the following photophysiological ranges were rejected: $200 < \text{absorption cross-section } (\sigma_{\text{PSII}}, \text{Å}^2) < 2000$ (as outlined in Ryan-Keogh and Robinson, 2021) and $0 < F_v/F_m < 0.65$. The latter cut-off was applied as the maximum observed F_v/F_m values for phytoplankton under optimum growth conditions were found in the literature to be ca. 0.65 and 0.70, dependent on the taxonomy (Juneau and Harrison, 2005; Suggett et al., 2009). (3) Furthermore, data were excluded if the Root Mean Square Error (RMSE) value was greater than the mean RMSE for each cruise.

2.1.2 Diurnal variability

To test whether Non-Photochemical Quenching (NPQ; Owens et al., 1980; Falkowski, 1997) significantly impacted daytime F_v/F_m , day (local sunrise to local sunset) and night (local sunset to local sunrise) F_v/F_m values were compared to each other for all cruises (S48, S49, S53, S54 and S55) combined, across each geographic zone (SAZ, PFZ, AZ and SACCZ) (Supplementary Table S3). Please refer to section 2.3.1. for how the statistical t-tests were performed.

2.1.3 Chl-a concentrations

Seawater samples (250-500 mL) were collected from the ship's continuous underway supply for Chl-a and filtered through a Whatman Glass Fiber Filter (GF/F) filter (nominal pore size 0.7 μm). The filter was extracted in 90% acetone for 12–24 hours in the dark at -20°C and measured on a Turner Designs 10AUTM

fluorometer (during the S48 cruise) and Turner Trilogy (all other cruises), calibrated with a Chl-a standard (Sigma Aldrich) following the non-acidification method (Welschmeyer, 1994).

2.2 Ancillary data

2.2.1 Surface seawater temperature (SST)

SST was continuously measured every minute during each cruise by a Seabird thermo-salinograph installed at the intake of the ship's underway scientific water supply.

2.2.2 Macronutrients

Samples for macronutrients nitrate (NO_3^-), silicate (Si(OH)_4) and phosphate (PO_4^{3-}) on S48 were manually analyzed on-board, following the methods described by Grasshoff et al. (1983) and Parsons et al. (1984). S49 macronutrient samples were analyzed similarly as above, with the exception of silicate, which was stored frozen at -20°C and later analyzed on a Lachat QuikChem 8500 series 2 Flow Injection Autoanalyzer (FIA) (Wolters, 2002; Egan, 2008). On S53, S54 and S55, nitrate and silicate were run on the Lachat QuikChem 8500 FIA while phosphate was run manually following the methods described by Grasshoff et al. (1983) and Parsons et al. (1984). The nitrate:phosphate and silicate:phosphate molar ratios, hereafter referred to as N:P and Si:P, were computed for each station per cruise with phosphate as the common denominator due to its long ocean residence time compared to other biologically limiting macronutrients and it being a traditional tracer (Bigg and Killworth, 1988).

2.2.3 Community structure

Samples were collected for High-Performance Liquid Chromatography (HPLC) to determine the photosynthetic pigment composition by filtering between 1000 mL and 2000 mL of seawater onto 25 mm diameter Whatman GF/F filters that were stored in liquid nitrogen (S48 and S49) or in a -80°C freezer (all other cruises) until further analysis on land. For S48 and S49, pigments were extracted in 90% acetone, aided by ultrasonification for a few seconds, the extract was centrifuged and analyzed by HPLC as described by Barlow et al. (1997). Samples from S48 were analyzed at the Department of Environmental Affairs (DEA), South Africa, while samples from S49 were analyzed at the National Oceanography Centre, Southampton (NOCS), UK. For S53, S54 and S55, pigments were extracted in 100% methanol, aided by the use of ultra-sonification for a few seconds. The extract was filtered and analysed at Laboratoire d'Océanographie de Villefranche-sur-Mer, France, according to Ras et al. (2008). Root square transformations were applied to the pigment composition data for standardization prior to cluster analysis utilizing multi-dimensional scaling to group samples as outlined by Gibberd et al. (2013). The community structure of phytoplankton was then determined from the

pigment ratios using Gibberd et al. (2013), and the CHEMTAX software (Mackey et al., 1996; Wright et al., 2010).

2.2.4 Diagnostic pigment ratios and the effective cell diameter (D_{eff}) index

The diagnostic pigment ratios described by Vidussi et al. (2001) were used to determine micro-, nano- and picophytoplankton contributions at each station. A representative particle size-structure index for each sample was then calculated by assuming a representative size for microphytoplankton (20 μm), nanophytoplankton (10 μm) and picophytoplankton (1 μm) (Thomalla et al., 2017). The contribution of each size class was multiplied by the representative cell diameter at each station and summed to calculate an effective cell diameter (D_{eff}) per station (Thomalla et al., 2017).

2.3 Statistical tests

2.3.1 t-tests

Data were grouped into daytime versus night-time (defined by local sunrise and sunset), season (early summer (December) and late summer (February)) and per zone (SAZ, PFZ, AZ, SACCZ) for each cruise (S48, S49, S53, S54 and S55) to determine: (a) day and night means of F_v/F_m for assessing diurnal variability, and (b) to assess the statistical significance between zones, years and seasons. The statistical significance was evaluated by making use of a Levene test to check for equal variances, where a standard student's t-test was used for data of equal variance or a Welch's t-test for when data was of unequal variances. The t-tests were performed to compare the mean F_v/F_m values as follows: (1) inter-zonal variability (differences between zones) (2) inter-annual variability (differences between years) and (3) intra-seasonal variability as a comparison of early (December) versus late (February) summer. Results of the t-tests are reported as statistically significant when $p < 0.05$, $p < 0.01$ or $p < 0.001$.

2.3.2 Principal Component Analysis

The F_v/F_m data were co-located with the 4-hourly ancillary data for each cruise, where a 15-minute mean interval was taken for F_v/F_m before and after each matching station in date, time, latitude and longitude to create a combined dataset of F_v/F_m and the ancillary data for all cruises. Worth noting is that since the F_v/F_m data were collected in 5-min averages and the ancillary data collected every 4 hours this co-located data set represents only a small subset of the total F_v/F_m data set ($n = 68$). After removing all missing values, a Principal Component Analysis (PCA) was performed using the Python package MLxtend (Raschka, 2018) for each co-located F_v/F_m and ancillary data parameter, i.e., SST, N:P, Si:P, the chosen dominant community structure (diatom:haptophyte ratio) and D_{eff} , as well as the bulk concentrations of nitrate, phosphate and silicate.

3 Results

3.1 Diurnal variability

In vivo fluorescence can vary over a diel cycle with suppressed Chl-a fluorescence values expected during the day compared to night. This is due to NPQ being a photoprotective process during daytime, whereby excess energy is dissipated as heat at the cost of fluorescence to avoid photo-oxidative damage under high irradiance (Owens et al., 1980; Falkowski, 1997). F_v/F_m measurements during the night reflect dark-adapted states and can be used to establish the effect of non-light-induced stress on the photosynthetic apparatus. Differences between day and night data were found to be significant ($p < 0.05$) for all zones (Figure 2), and as such, only the night data were used for further analysis for all zones.

3.2 Inter-zonal distribution and inter-annual variability

In this paper "inter-annual" refers to the comparison between the summer cruises. Overall, mean F_v/F_m values comprising all cruises were highest for the PFZ (0.24 ± 0.03 ; $p < 0.001$), followed by the AZ (0.23 ± 0.04), SAZ (0.22 ± 0.04) and the lowest for the SACCZ (0.18 ± 0.07 ; $p < 0.001$) (Figure 3; Table 1 and Supplementary Table S4). An investigation of inter-annual variability in F_v/F_m between each of the cruises for each zone showed that both the PFZ and SACCZ had particularly high inter-annual variability with most years being significantly different from each other (Tables 2B, D). The SACCZ was also characterized by higher SD's ($\pm 0.04 - \pm 0.10$)

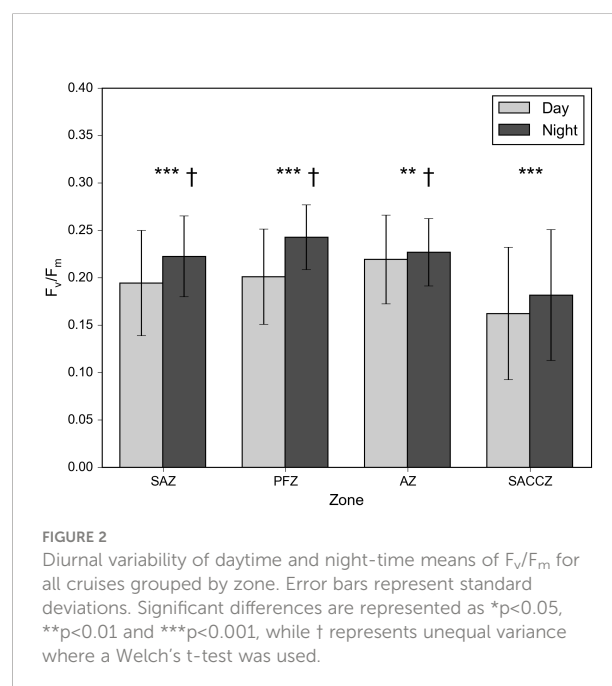


FIGURE 2
Diurnal variability of daytime and night-time means of F_v/F_m for all cruises grouped by zone. Error bars represent standard deviations. Significant differences are represented as * $p < 0.05$, ** $p < 0.01$ and *** $p < 0.001$, while † represents unequal variance where a Welch's t-test was used.

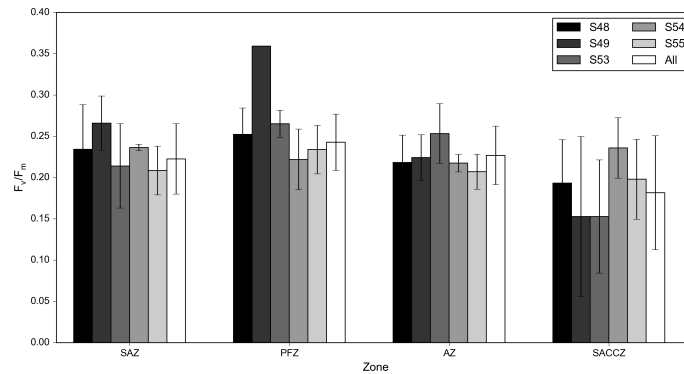


FIGURE 3 Inter-zonal distribution and inter-annual variability of the mean F_v/F_m . Error bars represent standard deviations. Note that S49 in the PFZ had too few data points to create a standard deviation ($n=1$).

TABLE 1 Inter-zonal variability: p-values from the t-tests conducted on the F_v/F_m for all cruises combined and compared per zone.

	SAZ	PFZ	AZ	SACCZ
SAZ		p<0.001†	0.18†	p<0.001†
PFZ			p<0.001	p<0.001
AZ				p<0.001†
SACCZ				

Statistically significant results ($p<0.05$) are highlighted in grey, with † representing unequal variance where a Welch’s t-test was used.

(Supplementary Table S5) compared to other zones ($\pm 0.003 - \pm 0.05$), indicative of a higher range of inter-annual variability. In the AZ, inter-annual variability was particularly low with the

majority of the cruises being similar, except S53 (Table 2C), which showed a higher mean F_v/F_m (0.25 ± 0.04 , $p<0.001$) compared to all other cruises (0.21 - 0.22) (Supplementary Table S5). The SAZ was also characterized by relatively high inter-annual variability in F_v/F_m , most notably during S49 which was typically higher than all other years, except S54 (Table 2A).

3.3 Intra-seasonal variability

As the cruises extended over the entire summer season, intra-seasonal differences were investigated between early (December) and late (February) summer (i.e., excluding all data from January). Averaged across all zones and all cruises

TABLE 2 Inter-annual variability per zone: p-values from the t-tests conducted on the F_v/F_m per cruise in each zone (Figure 3).

(a) SAZ						(b) PFZ					
	S48	S49	S53	S54	S55		S48	S49	S53	S54	S55
S48		p<0.001†	0.17	0.95	p<0.01†	S48		n/a	p<0.001†	p<0.001	p<0.001
S49			p<0.001†	0.22	p<0.001	S49			n/a	n/a	n/a
S53				0.55	0.65†	S53				p<0.001†	p<0.001†
S54					0.18†	S54					p<0.05
S55						S55					
(c) AZ						(d) SACCZ					
	S48	S49	S53	S54	S55		S48	S49	S53	S54	S55
S48		0.42	p<0.001	0.82	0.08†	S48		p<0.001†	p<0.001	p<0.01	0.60
S49			p<0.01	0.30†	0.06	S49			0.99†	p<0.001†	p<0.001†
S53				p<0.001†	p<0.001	S53				p<0.001	p<0.001
S54					p<0.05	S54					p<0.05
S55						S55					

Statistically significant results ($p<0.05$) are highlighted in grey, with † representing unequal variance where a Welch’s t-test was used. The term n/a refers to where there is a lack of data to perform a test, i.e., the PFZ during S49.

(“All” in Figure 4A), the seasonal comparison of F_v/F_m was higher ($p < 0.05$) during early summer (December, 0.22 ± 0.04) than in late summer (February, 0.20 ± 0.07) (Supplementary Table S6). However, this was not reflected consistently in all the individual zones. Although the same tendency was observed in the SACCZ (i.e., higher F_v/F_m in December 0.18 ± 0.07), the opposite was observed in the PFZ and AZ, where higher F_v/F_m values were observed in February ($p < 0.001$, Supplementary Table S7). The SAZ, in contrast, showed no significant difference between December and February (Supplementary Table S7). Similarly, when scrutinized on a cruise-by-cruise basis (Figure 4B), intra-seasonal differences in F_v/F_m were inconsistent, with higher values ($p < 0.05$) observed in December during S49 and S53, whereas higher values were observed in February during S48 ($p < 0.001$) and S54, whilst no intra-seasonal changes were seen for S55 (Supplementary Table S6).

3.4 Investigating zonal, inter-annual and intra-seasonal co-variability between F_v/F_m and ancillary data

The ancillary data investigated here include SST, ambient macronutrient concentrations and ratios (N:P and Si:P) as well as indices of phytoplankton community structure (pigment ratios and effective cell diameter (D_{eff})). A summary of the mean values of these potential drivers per zone is available in Supplementary Table S4. For each significant difference observed in F_v/F_m between zones (inter-zonal, Table 1), cruises (inter-annual, Table 2) and December-February (intra-seasonal, Supplementary Tables S6, S7), the corresponding significant differences in ancillary data were similarly established. This means that ancillary data were only tested for significant differences if the F_v/F_m showed a significant difference. If a

significant difference in F_v/F_m was also observed in an ancillary parameter, it could be considered as co-varying. As such, a co-varying parameter could be considered as a possible direct or indirect driver of the observed variability in F_v/F_m . Likewise, if no difference was observed in the ancillary data, it was excluded as a potential driver of the observed variability in F_v/F_m .

3.4.1 Surface seawater temperature (SST)

The mean SST averaged over all cruises decreased from maximum values of $\sim 12^\circ\text{C}$ in the SAZ southward towards minimum values of $\sim 1^\circ\text{C}$ in the SACCZ (Figure 5A and Supplementary Table S4). SSTs were different ($p < 0.001$) between all the zones (Supplementary Table S8) and between some cruises within each zone (Supplementary Table S9). For example, inter-annual variability in SST was observed for S53 in the PFZ with lower ($p < 0.001$) SST ($\sim 6^\circ\text{C}$) compared to S54 and S55 ($7.2^\circ\text{C} - 7.4^\circ\text{C}$), and in the AZ with lower ($p < 0.001$) SST ($\sim 2^\circ\text{C}$) than S49, S54 and S55 ($3.3^\circ\text{C} - 3.8^\circ\text{C}$). SST was higher ($p < 0.001$) in the SACCZ during S54 ($\sim 2^\circ\text{C}$) compared to all the other cruises ($-0.1^\circ\text{C} - 1.2^\circ\text{C}$) and during S55 ($\sim 1^\circ\text{C}$) compared to S49, S53 and S54 ($-0.1^\circ\text{C} - 2.1^\circ\text{C}$) (Supplementary Tables S5, S9). Intra-seasonal differences in SST were inconsistent (i.e. late summer was not consistently warmer) considering individual zones and individual cruises. For example, lower ($p < 0.001$, Supplementary Table S7) SSTs were observed in early summer in the PFZ and AZ and during S49 ($p < 0.05$), while lower SSTs were seen during S48 in late summer ($p < 0.05$, Supplementary Table S6).

3.4.2 Macronutrient concentrations and macronutrient ratios

The macronutrient concentrations varied from the SAZ to the SACCZ (Figure 5B and Supplementary Table S4), where the nitrate concentrations increased from $7.1 \pm 5.2 \mu\text{mol L}^{-1}$ in the SAZ to $\sim 20 \mu\text{mol L}^{-1}$ in the PFZ and SACCZ. The phosphate concentrations were the lowest in the SAZ ($0.7 \pm 0.6 \mu\text{mol L}^{-1}$)

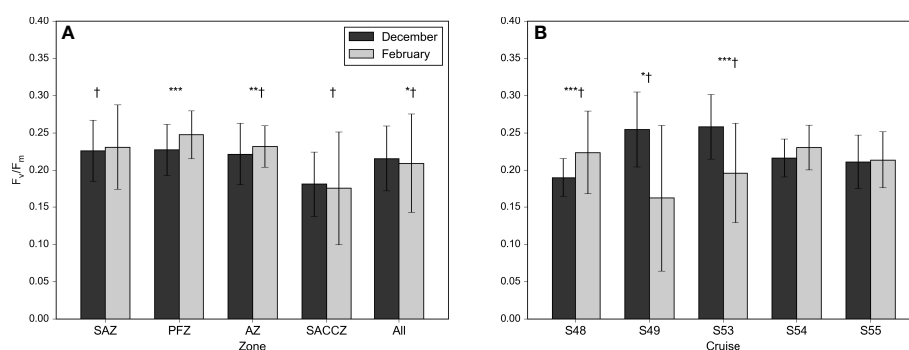


FIGURE 4

Intra-seasonal (early vs late summer) variability of F_v/F_m across (A) each zone and (B) per cruise in December and February. Error bars represent standard deviations. The overall mean F_v/F_m across all zones per season is shown as “All” in (A). Significant differences are represented as * $p < 0.05$, ** $p < 0.01$ and *** $p < 0.001$. Significant differences are represented as * $p < 0.05$, ** $p < 0.01$ and *** $p < 0.001$, while † represents unequal variance where a Welch’s t-test was used.

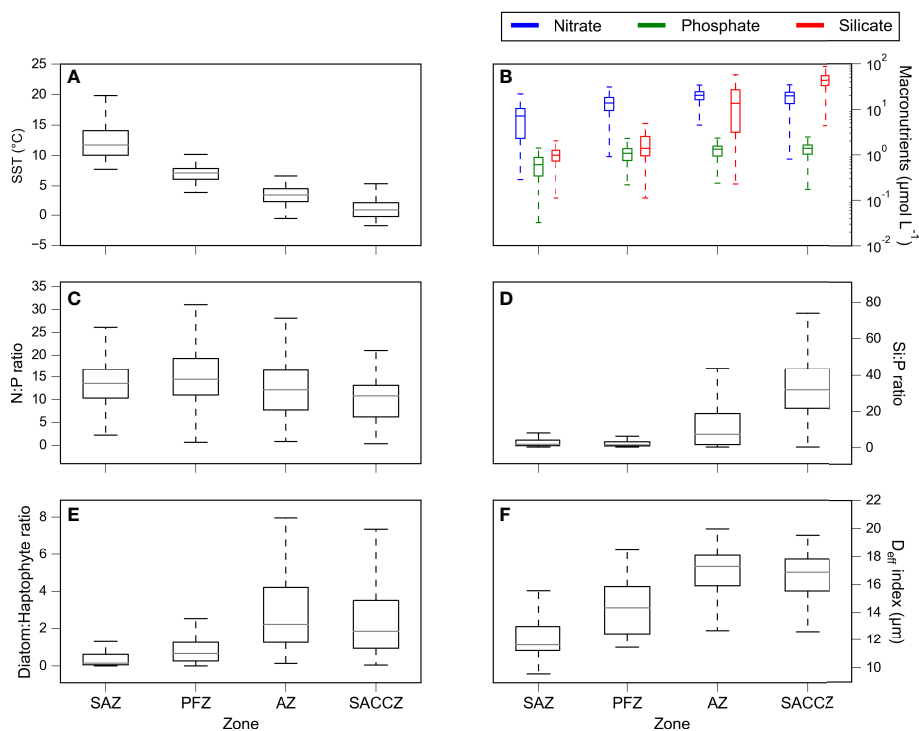


FIGURE 5

Ancillary parameters grouped per zone across all cruises for (A) Surface seawater temperature (SST) (°C), (B) Macronutrient concentrations ($\mu\text{mol L}^{-1}$) plotted on a logarithmic scale, (C) Nitrate:Phosphate (N:P) (mol:mol) and (D) Silicate:Phosphate (Si:P) (mol:mol), (E) Diatom:Haptophyte ratio (% contribution to Chl-a) and (F) the phytoplankton effective diameter (D_{eff}) index (μm). Boxplots represented as 25th and 75th percentile with median. Error bars represent standard deviations.

and increased to $\sim 1.4 \mu\text{mol L}^{-1}$ for the remaining three zones, substantiating phosphate as a good reference point to study the changes in nitrate and silicate as nutrient ratios, i.e. N:P and Si:P ratios. The silicate concentrations, however, steadily increased from $1.2 \pm 0.8 \mu\text{mol L}^{-1}$ in the SAZ to $45.7 \pm 18.5 \mu\text{mol L}^{-1}$ in the SACCZ.

The mean molar N:P ratios (mol:mol) for all cruises combined across all zones ranged from 10.7 ± 6.7 in the SAZ to 13.6 ± 6.8 in the SACCZ (Figure 5C and Supplementary Table S4). Significant differences were observed for the N:P ratios between all zones ($p < 0.05$), except between the PFZ and SACCZ (Supplementary Table S10). Inter-annual differences in N:P ratios were observed between the cruises, notably in the PFZ, AZ and SACCZ for S53 (Supplementary Table S11). S53 stood out with mean N:P ratios that were significantly lower in the PFZ (7.5 ± 3.4 , $p < 0.001$), compared to S48, S54 and S55 (13.2 - 15.4), and significantly lower in the AZ compared to all other cruises (6.4 ± 6.7 , $p < 0.001$). In the SACCZ, S53 was lower (9.5 ± 9.3 , $p < 0.001$) than S48, S54 and S55 (13.6 - 16.2) and higher during S55 (16.2 ± 6.5 , $p < 0.01$) compared to S49, S53 and S54 (9.5 - 14.1). Intra-seasonal differences of higher N:P ratios during early summer (December) were only observed in the AZ ($p < 0.01$) (Supplementary Table S7) and during S48

($p < 0.001$), while a lower N:P ratio was seen in December during S49 ($p < 0.01$) (Supplementary Table S6).

The mean molar Si:P ratios (mol:mol) for all cruises (Figure 5D) showed substantial latitudinal variability with low ratios in the SAZ (4.1 ± 7.4) and PFZ (3.8 ± 10.7), increasing to 11.6 ± 13.3 in the AZ and as high as 33.9 ± 24.6 in the SACCZ (Supplementary Table S4). Inter-zonal differences were significantly higher for Si:P ratios between the SACCZ and all other zones ($p < 0.001$) and between the PFZ and the AZ ($p < 0.001$) (Supplementary Table S12). Inter-annual differences were again observed during S53 ($p < 0.05$, Supplementary Tables S5, S13), with lower ratios in the PFZ (0.6 ± 0.3 , $p < 0.05$) compared to cruises S48, S54 and S55 (1.5 - 7.0) and in the AZ (7.5 ± 12.1 , $p < 0.001$) compared to S48, S54 and S55 (11.7 - 14.7). Lower Si:P ratios were seen in the SACCZ for S53 (26.4 ± 23.3 , $p < 0.001$) compared to S54 and S55 (38.1 - 51.7), and for S55 (51.7 ± 33.4 , $p < 0.01$) compared to S49, S53 and S54 (18.7 - 38.1). In contrast, Si:P ratios for S54 were higher (38.1 ± 17.7 , $p < 0.01$) than for all the other cruises (18.7 - 26.4), but lower ($p < 0.001$) than during S55 (51.7). Intra-seasonal differences with lower Si:P ratios in December compared to February were only observed in the AZ ($p < 0.01$) and on S49 ($p < 0.001$) (Supplementary Tables S7 and S6).

3.4.3 Community structure: pigment ratios

The two dominant phytoplankton groups across all cruises and all zones measured by their contribution to total Chl-a (in %), were diatoms (3% - 67%) and haptophytes (22% - 46%) (Supplementary Figure S1A). All other groups typically contributed less than 10%, e.g., dinoflagellates (4% - 7%), Prasinophytes (1% - 9%) and Cryptophytes (<5%), or showed higher contributions only in one particular zone, e.g. Chlorophytes (27%) and *Synechococcus* (12%) in the SAZ. As such, a focus was placed on the diatom to haptophyte ratio, which provides a single value index of change in community structure. The diatom:haptophyte ratio increased southwards from 0.4 ± 0.6 in the SAZ to 1.0 ± 1.1 in the PFZ, 5.0 ± 12.0 in the AZ and then decreased to 2.7 ± 2.6 in the SACCZ (Figure 5E and Supplementary Table S4). Inter-zonal differences in diatom:haptophyte ratios were significantly lower ($p < 0.05$) in the SAZ compared to both the PFZ and SACCZ, and lower ($p < 0.001$) in the PFZ compared to the SACCZ (Supplementary Table S14). In addition, inter-annual differences in the diatom:haptophyte ratio were evident in the PFZ and SACCZ, where for example, in the PFZ S54 (3.3 ± 0.9) was higher ($p < 0.01$) than S48, S53 and S55 (0.5 - 0.9) (Supplementary Tables S5 and S15). In the SACCZ, the diatom:haptophyte ratio was higher ($p < 0.001$) during S53 (2.0 ± 1.6) compared to S55 (3.3) (Supplementary Tables S5 and S15). Both the SAZ and AZ showed no significant inter-annual differences between cruises. Intra-seasonal comparisons of the diatom:haptophyte ratio in each zone showed no significant differences (Supplementary Table S7), whilst intra-seasonal variability in an inter-annual context indicated significantly higher ratios ($p < 0.01$) during December on S53 compared to February (Supplementary Table S6).

3.4.4 Effective cell diameter (D_{eff}) index

Phytoplankton were grouped into the following size fractions: microphytoplankton ($f_{\text{micro}} > 20 \mu\text{m}$), nanophytoplankton ($2 \mu\text{m} > f_{\text{nano}} > 20 \mu\text{m}$) and picophytoplankton ($f_{\text{pico}} < 2 \mu\text{m}$) (Supplementary Figure S1B). The f_{pico} (0.3% - 6%) and f_{nano} (29% - 67%) fractions decreased southwards, dominating in the SAZ and PFZ, whereas f_{micro} (26% - 70%) increased southward to dominate in the AZ and SACCZ. In order to attain a single value index to represent community size structure, an effective cell diameter (D_{eff}) was calculated for each station (see methods section 2.2.4). The D_{eff} index increased southwards from $12.1 \pm 2.3 \mu\text{m}$ in the SAZ to $14.3 \pm 1.9 \mu\text{m}$ in the PFZ and then up to $17.0 \pm 1.6 \mu\text{m}$ in the AZ, remaining similar in the SACCZ ($16.6 \pm 1.7 \mu\text{m}$) (Figure 5F and Supplementary Table S4). D_{eff} was significantly lower ($p < 0.001$) in the SAZ compared to both the PFZ and SACCZ and was lower in the PFZ compared to both the AZ and SACCZ ($p < 0.001$) (Supplementary Table S16). In the PFZ, D_{eff} values on S48 were lower (13.0 ± 1.2 ; $p < 0.05$) than on S53 (14.7 ± 1.9), while in the SACCZ, the S49 D_{eff} values were lower (15.2 ± 1.5 ; $p < 0.05$) than during S48, S54 and S55 ($16.3 - 17.1$) (Supplementary Tables S5 and

S17). No inter-annual differences were evident in D_{eff} in the SAZ or AZ. Intra-seasonal differences were evident with higher D_{eff} in December in the PFZ and AZ (Supplementary Table S7), and with higher D_{eff} in December on S53 (Supplementary Table S6).

3.5 Co-variability between the ancillary parameters and F_v/F_m

3.5.1 Inter-zonal co-variability

SST significantly differed between all zones and co-varied inter-zonally, similar to F_v/F_m (Supplementary Table S4). Zonal differences in N:P and Si:P ratios also co-varied with changes in F_v/F_m for the majority of zones, except for similarities in the PFZ and SACCZ for N:P ratios and in both the PFZ and the SAZ for Si:P ratios (Supplementary Tables S10 and S12). Changes in community structure, i.e., both the diatom:haptophyte ratio and D_{eff} , co-varied with changes in F_v/F_m between zones, except between the AZ and SACCZ for which they were similar (Supplementary Tables S14 and S16).

3.5.2 Inter-annual co-variability

Ancillary parameters that matched the inter-annual significant differences in F_v/F_m are SST and both macronutrient ratios, mainly in the PFZ, AZ and SACCZ (Table 2 and Supplementary Tables S5, S11, S13). The diatom:haptophyte ratios and D_{eff} , on the other hand, matched the inter-annual significant differences in F_v/F_m in the PFZ and SACCZ (Table 2 and Supplementary Tables S5, S15, S17). In the PFZ, significant differences in SST, as well as macronutrient ratios co-varied with a significantly higher mean F_v/F_m , most notably for S53, which had the lowest SST and nutrient ratios when compared to most of the other cruises. In the AZ, however, the lowest SST and N:P ratios for S53 coincided with the highest mean F_v/F_m . In the SACCZ, the highest mean SST and a high mean Si:P ratio co-varied with the high mean F_v/F_m for S54 compared to all other cruises, and the lowest mean N:P ratio for S53 compared to cruises S48, S54 and S55. The diatom:haptophyte ratio showed only a few significant inter-annual differences ($p < 0.05$), such as in the PFZ and in the SACCZ (Supplementary Table S15).

3.5.3 Intra-seasonal co-variability

Differences assessed between all early and all late summer data, i.e., comparing December to February for all cruises across all zones combined, showed that both the N:P and Si:P ratios did not vary (Supplementary Table S6). Ancillary parameters which matched intra-seasonal differences observed in F_v/F_m included SST and D_{eff} index in the PFZ and AZ, as well as the N:P and Si:P ratio only in the AZ (Supplementary Table S7). Ancillary parameters, which matched intra-seasonal differences observed in F_v/F_m , among the years were SST and N:P ratios during S48

and S49; Si:P ratios only during S49; as well as the diatom:haptophyte ratio and D_{eff} index on S53 (Supplementary Table S6).

3.6 Principal Component Analysis between ancillary data and F_v/F_m

Despite the limited number of F_v/F_m data points that were co-located with ancillary data, when combined across all zones and seasons there was a sufficient sample size ($n = 68$) to perform a PCA analysis to identify the ancillary data which showed the strongest co-variance (Supplementary Figure S2). The sum of the first two principal components in the PCA explained 68% of the total variance in F_v/F_m . The grouping of the variables within each quadrant shows F_v/F_m to be in the opposite quadrant to the silicate concentration and the N:P and Si:P ratios, whilst SST was in the neighboring quadrant opposite to the nitrate and phosphate concentrations and the community structure indices.

4 Discussion

Active Chl-a fluorescence provides instantaneous, high-resolution spatial and temporal information on the response of phytoplankton to physiological stress caused by the local environment (Hughes et al., 2018). Here, we focus on F_v/F_m as an indicator of phytoplankton photosynthetic efficiency and examine the inter-zonal, inter-annual and intra-seasonal variability in F_v/F_m distribution across the Atlantic SO in summer. In addition, we investigate zonal, inter-annual and intra-seasonal co-variability in ancillary parameters to elucidate the possible direct and indirect drivers of variability in F_v/F_m . Finally, we use a PCA on a subset of co-located F_v/F_m and ancillary data to further assess the dominant drivers of overall F_v/F_m variability (i.e., across all years, zones and for all three months of summer).

4.1 Zonal, inter-annual and intra-seasonal variability in F_v/F_m

F_v/F_m exhibited large-scale spatial variability between the zones and was the highest in the PFZ (0.24 ± 0.03). These values are similar to those previously reported for other open ocean regions such as those near the Kerguelen Plateau (0.2 - 0.4; Timmermans et al., 2008), but much lower than those observed downstream of sub-Antarctic islands (0.5 - 0.6; Moore et al., 2007; Timmermans et al., 2008). High F_v/F_m in the PFZ implies efficient photosynthesis that was the least constrained by environmental conditions. Optimal environmental summer conditions such as these are likely to result in higher rates of production for the PFZ and hence, possibly higher carbon

drawdown in the region (Uitz et al., 2006). On the other hand, F_v/F_m in the SACCZ was the lowest (0.18 ± 0.07), which potentially implies inefficient photosynthesis that was most likely limited by a combination of light and/or nutrients. In instances such as this, primary production is typically curtailed, leading to a potentially constrained biological carbon pump (Hardman-Mountford et al., 2013). However, Chl-a concentrations for this zone were the highest (Supplementary Figure S3), which implies that despite sub-optimal efficiency in photosynthesis (from possible light limitation or a combination of other factors), rates of production and biomass accumulation were substantial and unlikely to curtail export.

When averaged across all zones and cruises, F_v/F_m was typically higher in early summer when compared to late summer (Figure 5, Supplementary Table S3). This is in line with our understanding of seasonal nutrient limitation (in particular with regards to iron) following biological utilization and is in accordance with the literature (Deppeler and Davidson, 2017; Ryan-Keogh et al., 2018; Mtshali et al., 2019). However, when zones (and cruises) were interrogated on an individual basis this tendency was not consistently reflected. For example, no intra-seasonal difference was evident in the SAZ and SACCZ when all cruises were combined (Supplementary Table S4) and a higher F_v/F_m was instead observed in late summer in the PFZ and AZ. Similarly, when all zones were combined, although higher F_v/F_m was observed in early summer on S49 and S53, the opposite was true for S54 with no discernible difference on S54. This inconsistency of an intra-seasonal decline in F_v/F_m in late summer highlights the likelihood of a dynamic interplay of sub-seasonal variability in nutrient and light variability in addition to the phytoplankton community response that together determines the characteristics in F_v/F_m .

Different zones displayed different degrees of inter-annual variability in F_v/F_m . Using inter-annual variability as an approach for zonal characterization provides a dynamic understanding of phytoplankton regionalization that relies on underlying physical drivers in addition to climatological means (Thomalla et al., 2011). The SACCZ (and to a lesser extent the PFZ) had particularly high inter-annual variability in F_v/F_m , with most cruise occupations being significantly different from each other, suggesting that changes in the local environment between annual occupations were strongly impacting F_v/F_m . In addition, the highest range of SD in the SACCZ is indicative of the highest degree of inter-annual variability in F_v/F_m . Regions that are characterized by a high degree of inter-annual variability (i.e., the SACCZ and PFZ) are more likely to be influenced by sub-seasonal forcing of the nutrient and light supply e.g., through storm interactions that drive event scale variability in the MLD (Thomalla et al., 2011). F_v/F_m in the AZ on the other hand showed much lower inter-annual variability with mean values that were surprisingly similar for four of the five cruise occupations. Zones with particularly low inter-annual variability in F_v/F_m such as the AZ are more likely to be phase locked with

the seasonal forcing of light and nutrients from a seasonal shoaling of the MLD (Thomalla et al., 2011). This does not mean that nutrients or light are not impacting F_v/F_m but merely that it is unlikely to vary sufficiently on intra-seasonal timescales to strongly influence inter-annual variability in F_v/F_m .

4.2 Investigating potential drivers of spatial and temporal variability in phytoplankton photophysiology

Iron plays a fundamental role in the photosynthetic process (Raven et al., 1999) and typically has a direct effect on F_v/F_m , which is why it is often referred to as the master variable. F_v/F_m variability in regions such as the SO that typically experience iron limitation, with low dissolved iron (DFe) concentrations drive low F_v/F_m . Hence, some of the low F_v/F_m results could be linked to iron stress, for e.g., in the SAZ, where F_v/F_m was lower in late summer as would be expected from biological utilization following the spring bloom (Deppeler and Davidson, 2017; Ryan-Keogh et al., 2018; Ryan-Keogh et al., ; Mtshali et al., 2019). However, without local DFe data, we are unable to adequately investigate its influence on F_v/F_m variability. A zonal comparison of F_v/F_m with DFe concentrations from the GEOTRACES data set (GEOTRACES Intermediate Data Product Group, 2021) did, however, show the SACCZ to be characterized by the highest concentrations of DFe (Supplementary Figure S4) but the lowest F_v/F_m (Figure 3). This implies that photosynthesis in this zone was unlikely to be iron-limited, but that F_v/F_m was more likely to be constrained by a combination of alternative drivers. Iron measurements were conducted as part of incubation studies on S54 and S55 with reported results suggesting that primary production was affected by iron-limitation during summer (Ryan-Keogh et al., 2017;

Ryan-Keogh et al., 2018; Viljoen et al., 2018), with some potential iron-light co-limitation in the PFZ (Viljoen et al., 2018).

In the following section, the characteristics of zonal, inter-annual and intra-seasonal variability in F_v/F_m are investigated in the context of co-variability of the available ancillary data (summarized in Figure 6) in order to determine whether or not the ancillary parameter could be considered as a possible direct or indirect driver of F_v/F_m .

4.2.1 The dynamics between SST and F_v/F_m variability

At a global level, SST does not directly drive F_v/F_m , since both high and low F_v/F_m can be found in both tropical and polar waters. At a local level, however, positive correlations have been observed between SST and F_v/F_m , e.g., for dinoflagellates in the East China Sea (Shen et al., 2016). In our transects across the SO, a southward decrease in SST coincided with a zonal decrease in F_v/F_m (Supplementary Table S4), supporting the understanding that SST impacts the metabolic balance of phytoplankton (Maxwell and Johnson, 2000; Finkel et al., 2010; Marañón et al., 2018), which can indirectly impact the F_v/F_m signature. However, despite the general latitudinally co-varying trends, warmer SO waters did not always host higher F_v/F_m and colder SO waters did not always host lower F_v/F_m . For example, significantly warmer SSTs were observed in the SAZ compared to the AZ, but the F_v/F_m was nonetheless similar. Also, colder SSTs on S53 in the PFZ and AZ did not correspond to lower F_v/F_m . The response in F_v/F_m following changes in SST between early and late summer also varied. For example, on S48 higher December than February SSTs was accompanied by lower F_v/F_m , while on S54 lower December than February SSTs was accompanied by higher F_v/F_m . Nonetheless, when considering all years combined in the PFZ and AZ, December SSTs was

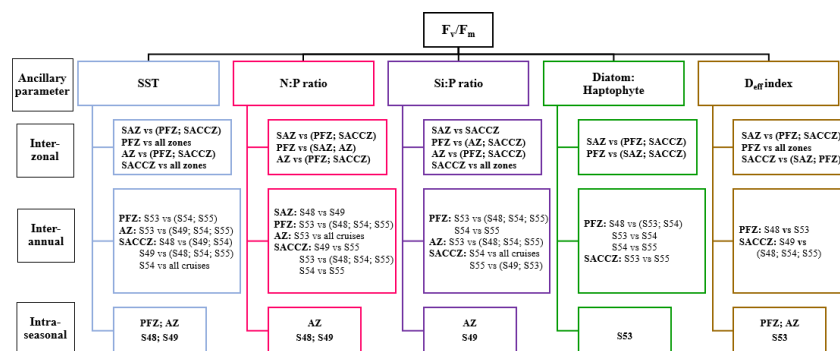


FIGURE 6

Schematic summary of the potential co-varying parameters (Surface seawater temperature, SST; Nitrate:Phosphate, N:P; Silicate:Phosphate, Si:P; Diatom:Haptophyte ratio and phytoplankton effective diameter (D_{eff}) index) of F_v/F_m (where F_v/F_m was different at $p < 0.05$), showing inter-zonal, inter-annual and intra-seasonal changes that matched changes in F_v/F_m . The zones/cruises before "vs" were different to each of the zones/cruises after "vs". Note all significant differences are shown where $p < 0.05$.

significantly lower than for February, which coincided with significantly lower F_v/F_m . In summary, although changes in SST and F_v/F_m often co-vary, the response with SST was not consistent at inter zonal, inter-annual or intra-seasonal scales. This highlights the important understanding that other drivers are at play and that any relationship with SST is not direct but rather a secondary reflection of an imbalance in cellular metabolism.

4.2.2 The impact of macronutrients on F_v/F_m variability

SO phytoplankton are known to respond to changes in their chemical environment through an altered photosynthetic response (i.e. F_v/F_m response to nutrient stress) and/or a community structure response that favors particular species under those conditions, which in turn drives an indirect secondary response in F_v/F_m (e.g. [Suggett et al., 2009](#)). Ambient nitrate or phosphate concentrations are generally not considered to be limiting in the SO ([Sedwick et al., 2002](#)), which is in agreement with our measured ambient nutrient data ([Supplementary Table S4](#)). As such, and due to phosphate remaining relatively constant, we instead emphasized the role of variability in ambient macronutrient ratios in order to reflect preferential or limited acquisition and drawdown, e.g., as a result of community adjustments or iron limitation in the case of N:P ratios ([Schoffman et al., 2016](#)). N:P ratios covaried with F_v/F_m for all zones except the PFZ and SACCZ, while on an inter-annual basis mainly in the PFZ, AZ and SACCZ during S53 and intra-seasonally in the AZ and during S48 and S49 ([Figure 6](#)). The PCA results similarly show that the N:P ratio was in the direct opposite quadrant to F_v/F_m , suggesting that the observed significant zonal, inter-annual and intra-seasonal co-variability in F_v/F_m and N:P ratios could be the result of driver response. However, based on the understanding that nitrate uptake is curtailed under iron limiting conditions, due to the high iron demand for nitrate reductase ([Timmermans et al., 1994](#)), it is possible that these relationships observed in co-variability and PCA regressions (between F_v/F_m and N:P ratios) are instead a secondary signature of iron limitation, i.e., high N:P ratios under iron limiting conditions being reflected in low F_v/F_m ratios.

Silicate, on the other hand, is considered to be limiting to diatoms, particularly towards the end of the growing season, most notably north of the PF ([Hutchins et al., 2001](#); [Boyd et al., 2010](#)). Our results supported this understanding with a zonal distribution in both the ambient silicate and the Si:P ratios, which increased significantly south in the AZ and SACCZ ([Figures 5B, D](#); [Supplementary Table 4](#)). A response in F_v/F_m to low Si:P ratios could reflect an indirect community response to low silicate conditions limiting the production of diatoms who typically express higher F_v/F_m than flagellates ([Suggett et al., 2009](#)). However, were this the case, a characteristically lower F_v/F_m would be anticipated in low Si:P diatom-dominated waters north of the PF, which was not the case. This lack of consistency

in any directional change in F_v/F_m being associated with macronutrient ratios was similarly observed inter-annually as well as intra-seasonally. This implies a more dominant role of other factors (e.g. cold temperatures / low light) in driving low F_v/F_m south of the PF.

4.2.3 The impact of community structure and cell size on F_v/F_m variability

As discussed previously, changes in phytoplankton community structure impact the baseline F_v/F_m ([Suggett et al., 2009](#)), with diatoms having a higher F_v/F_m than other phytoplankton groups. The increase in the diatom:haptophyte ratio and D_{eff} between the SAZ and PFZ indeed corresponded to such a significant increase in F_v/F_m , which is in line with expected changes that reflect the characteristic of higher F_v/F_m associated with larger diatom cells when conditions are favorable (i.e. not light or nutrient-limited) ([Boyd et al., 2010](#); [Koch et al., 2019](#)). However, the diatom:haptophyte ratio and D_{eff} continued to increase between the PFZ and SACCZ, but the F_v/F_m decreased, while similar community structure indices were observed between the AZ and SACCZ despite a significant decrease in F_v/F_m . These results imply that on the whole, zonal changes in F_v/F_m are not strongly influenced by community structure (as indexed by pigment ratios and D_{eff}), or that neither the diatom:haptophyte ratio nor D_{eff} is accurately reflecting the main shifts driving F_v/F_m . [Sosik and Olson \(2002\)](#), for example, found no significant differences in F_v/F_m between pico- and nanophytoplankton during late summer in the Pacific SO, despite an observed change in community composition toward nanophytoplankton cells south of the PF, thus favoring instead the role of other drivers.

When investigating the data on an inter-annual basis, a number of differences in the diatom:haptophyte ratio corresponded to expected differences in F_v/F_m . For example, lower F_v/F_m on S48 than S53 in the PFZ corresponded to lower diatom:haptophyte ratios. Similarly, in the SACCZ the highest F_v/F_m which was observed during S54, corresponded to a significantly higher diatom:haptophyte ratio. The same was, however, not true for D_{eff} which was relatively consistent over the years, with almost no influence evident on inter-annual F_v/F_m variability. On the other hand, intra-seasonal patterns were observed in the community structure indices of both D_{eff} and the diatom:haptophyte ratio which decreased (in all instances) from early to late summer, consistent with an expected phytoplankton community response to seasonal declines in nutrients ([Hutchins et al., 2001](#)). Changes in F_v/F_m , however, varied per zone and per year with only the SACCZ (all years) and S53 (all zones) showing a coincident seasonal decline in F_v/F_m . Similar to the role of macronutrients, it appears that although we are seeing sensible relationships between changes in F_v/F_m in response to changes in community structure, the lack of consistency suggests that additional factors are concurrently at play.

4.3 The particular case of S53 and S49

Examination of inter-annual variability within the zones showed S53 to be the only year displaying significant differences in F_v/F_m along with SST, N:P and Si:P ratios mainly for the PFZ and AZ compared to all the other cruises (Figure 6). As such, this year provides a unique test case for investigating the possible inter-annual co-variability in F_v/F_m . To begin with, S53 stood out as expressing the second-largest intra-seasonal variability in F_v/F_m (i.e., the second biggest decline in F_v/F_m between December and February), which coincided with a significant decline in both community structure indices (diatom:haptophyte ratio and D_{eff} index). S53 was also notable in displaying the highest mean F_v/F_m in the AZ compared to all other cruises, but counterintuitively showed the lowest SST and nutrient ratios. Finally, in the SACCZ, S53 showed a low mean F_v/F_m coincident with the lowest SST and N:P ratio. In summary, S53 was certainly a unique year, and although it was not always possible to reconcile variability in F_v/F_m with an anticipated driver response, it nonetheless highlighted the important role of community structure, SST and N:P influencing inter-annual variability in F_v/F_m .

S49 also stood out as a year with particularly high F_v/F_m in the SAZ and particularly low F_v/F_m in the SACCZ, as well as the largest intra-seasonal variability (i.e., the biggest decline in F_v/F_m between December and February). As such, we similarly focus on this cruise to see if it can shed light from a co-varying response perspective (Figure 6). In the SAZ, the highest F_v/F_m during S49 coincided with high SST, the lowest N:P ratio, the highest diatom:haptophyte ratio and the largest phytoplankton cell sizes (D_{eff}), implying that despite the low Si:P ratios large diatoms were primarily responsible for high F_v/F_m observed in the SAZ during S49. In the SACCZ, S49 exhibited low mean F_v/F_m coincident with the lowest diatom:haptophyte ratio and D_{eff} , indicative of a possible role for small cells driving low F_v/F_m .

Climate variability associated with an increase in the positive phase of the Southern Annular Mode (Henson et al., 2010; Swart et al., 2014; Marshall et al., 2018) is considered the clearest and most persistent change in Southern Hemisphere climate in the last half century (Polvani et al., 2011) eliciting a poleward shift and increase in the intensity of the westerly winds. Interestingly, the Southern Annular Mode index prior to S49 and S53 was lower compared to all other years (Supplementary Figure S5) (Climate Data Sets, 2022). This could have impacted environmental conditions and subsequently accounted for inter-annual variability in F_v/F_m during those particular years, highlighting the important role that the intensity of the westerly winds likely plays in influencing inter-annual variability of environmental drivers.

4.4 Complex interactions rather than single factors affect photophysiology

In many ways it is unsurprising that the ancillary parameter analyses did not typically reveal a dominant

candidate for influencing zonal, inter-annual or intra-seasonal variability in F_v/F_m . This is because there are a multitude of physio-chemical and biological drivers simultaneously impacting phytoplankton photosynthetic efficiency. As such, it is possible that multiple drivers can have an antagonistic impact on F_v/F_m such that the net effect may be zero. One example is the decrease in F_v/F_m in the AZ compared to the PFZ, despite higher Si:P and diatom:haptophyte ratios and larger cell sizes (D_{eff}), demonstrating a possible indirect influence of cold SSTs that suppress any positive response in F_v/F_m to favorable nutrients and community structure adjustments. This complexity is further substantiated with similar F_v/F_m in the SAZ and AZ despite significant differences in all drivers, while no single driver (from those studied here) could account for the significantly higher F_v/F_m observed in the PFZ compared to all other zones. These examples (and the case of S53 in the AZ) in which ancillary parameters cannot always justify the changes seen in F_v/F_m highlights the complex interplay between direct and indirect drivers of phytoplankton physiology (including ones not specifically addressed in this study e.g., iron) acting simultaneously to impact (or not) F_v/F_m variability.

5 Conclusion

Relatively little is known about the temporal and spatial variability of F_v/F_m and its biogeochemical controls in the higher latitudes (Deppeler and Davidson, 2017). This *in situ* study spans the full latitudinal extent of the Atlantic SO during five summer voyages (2008 – 2016) to assess zonal, inter-annual and intra-seasonal variability in phytoplankton photosynthetic efficiency, F_v/F_m . Zonal variability showed that the PFZ had the highest F_v/F_m , whilst the SACCZ had the lowest. This implies efficient photosynthesis in the PFZ that was the least constrained by environmental conditions and the most likely to generate higher rates of production positively impacting the BCP. Strong inter-annual variability in F_v/F_m was observed in the SACCZ and PFZ, with most years being significantly different, while the AZ exhibited very low inter-annual variability in F_v/F_m with only one year being different from the remaining four. This zonal investigation of inter-annual variability provides a dynamic understanding of phytoplankton regionalization in response to the characteristics of the underlying drivers, which are either strongly seasonal (expressed as low inter-annual variability) or highly variable i.e., more likely influenced by sub-seasonal forcing of the nutrient and light supply (expressed as high inter-annual variability). Intra-seasonal differences in F_v/F_m between early and late summer reflected seasonal nutrient limitation following biological utilization when averaged across all zones and cruises. However, this response was not consistent when considered per zone or per cruise highlighting the

likelihood of a dynamic interplay of sub-seasonal variability of environmental drivers. The characteristics of variability were investigated in the context of five biogeochemical ancillary data sets. Although variability appeared to be linked to SST, nutrient ratios and community structure depending on whether the data were grouped per zone or per cruise, no consistent patterns were evident in any single driver-response relationship. These results highlight the complex interplay between eco-physiological drivers and their photophysiological responses, which act simultaneously and oftentimes antagonistically making it difficult to detect a single driver influence from the net effect. This study alludes to how climate change may alter the impact of various environmental factors on phytoplankton photophysiology and, by extent, primary production and the BCP. More *in situ* studies on the drivers of photophysiology, including further potential key drivers such as iron, will provide a broader understanding of the factors limiting phytoplankton primary production in the SO, as well as assist in predicting how phytoplankton will respond to future conditions that are associated with climate change. Such information is vital for accurately predicting the future role of the SO in the global uptake and regulation of atmospheric CO₂.

Data availability statement

The datasets presented in this study can be found in online repositories. The names of the repository/repositories and accession number(s) can be found below: <https://zenodo.org/record/6989253>; Zenodo, 10.5281/zenodo.6989253.

Author contributions

ST and TR-K conceptualized the study. AS and TR-K performed the data analysis and produced the figures. AS wrote the initial manuscript. ST, SF, AS, and TR-K contributed to the study design, interpretation of the results and writing of the manuscript. All authors contributed to the article and approved the submitted version.

References

- Arrigo, K. R., Mills, M. M., Kropuenske, L. R., van Dijken, G. L., Alderkamp, A. C., and Robinson, D. H. (2010). Photophysiology in two major southern ocean phytoplankton taxa: photosynthesis and growth of phaeocystis antarctica and fragilariopsis cylindrus under different irradiance levels. *Integr. Comp. Biol.* 50, 950–966. doi: 10.1093/icb/icq021
- Arrigo, K. R., Robinson, D. H., Worthen, D. L., Dunbar, R. B., DiTullio, G. R., VanWoert, M., et al. (1999). Phytoplankton community structure and the drawdown of nutrients and CO₂ in the southern ocean. *Science* 283, 365–367. doi: 10.1126/science.283.5400.365
- Arrigo, K. R., van Dijken, G. L., and Bushinsky, S. (2008). Primary production in the Southern Ocean 1997–2006. *J. Geophys. Res. Ocean* 113 (C8). doi: 10.1029/2007JC004551
- Barlow, R. G., Cummings, D. G., and Gibb, S. W. (1997). Improved resolution of mono- and divinyl chlorophylls a and b and zeaxanthin and lutein in phytoplankton extracts using reverse phase c-8 HPLC. *Mar. Ecol. Prog. Ser.* 161, 303–307. doi: 10.3354/meps161303
- Bigg, G. R., and Killworth, P. D. (1988). Conservative tracers and the ocean circulation. *Philos. Trans. R. Soc. London. Ser. A Math. Phys. Sci.* 325, 177–187. doi: 10.1098/rsta.1988.0050

Funding

AS, ST and TR-K were supported through the CSIR's Southern Ocean Carbon-Climate Observatory (SOCCO) Programme (<http://socco.org.za/>) funded by the Department of Science and Innovation (DST/CON 0182/2017) and the CSIR's Parliamentary Grant. We would like to acknowledge funding received from a number of grants from the National Research Foundation, South Africa, grant numbers 110731 (SF), 91313 (SF), 118751 (ST) and 110729 (ST).

Acknowledgments

The authors would like to acknowledge the assistance of the Captain and crew on-board the SA Agulhas I and SA Agulhas II during the SANAE cruises: 48, 49, 53, 54 and 55. The authors would also like to thank the two reviewers for their constructive comments that contributed to refining this manuscript.

Conflict of interest

The authors declare that the research was conducted in the absence of any commercial or financial relationships that could be construed as a potential conflict of interest.

Publisher's note

All claims expressed in this article are solely those of the authors and do not necessarily represent those of their affiliated organizations, or those of the publisher, the editors and the reviewers. Any product that may be evaluated in this article, or claim that may be made by its manufacturer, is not guaranteed or endorsed by the publisher.

Supplementary material

The Supplementary Material for this article can be found online at: <https://www.frontiersin.org/articles/10.3389/fmars.2022.912856/full#supplementary-material>

- Boyd, P. W. (2002). Environmental factors controlling phytoplankton processes in the southern ocean. *J. Phycol.* 38, 844–861. doi: 10.1046/j.1529-8817.2002.t01-1-01203.x
- Boyd, P. W., Strzepek, R., Fu, F., and Hutchins, D. A. (2010). Environmental control of open ocean phytoplankton groups: Now and in the future. *Limnol. Oceanogr.* 55, 1353–1376. doi: 10.4319/lo.2010.55.3.1353
- Boyer, T. P., Antonov, J. I., Baranova, O. K., Coleman, C., Garcia, H. E., Grodsky, A., et al. (2013). World ocean database 2013. Silver Spring, MD: National Oceanographic Data Center, 208pp. (NOAA Atlas NESDIS, 72). doi: 10.25607/OBP-1454
- Brody, S. R., and Lozier, M. S. (2014). Changes in dominant mixing length scales as a driver of subpolar phytoplankton bloom initiation in the north Atlantic. *Geophys. Res. Lett.* 41, 3197–3203. doi: 10.1002/2014GL059707
- ClimateDataguide.ucar.edu (2022) *Climate data sets* | NCAR - climate data guide. Available at: <https://climatedataguide.ucar.edu/climate-data>.
- Cullen, J. J., and Davis, R. F. (2003). The blank can make a big difference in oceanographic measurements. *Limnol. Oceanogr. Bull.* 12, 29–35. doi: 10.1002/lob.200413229
- de Baar, H. J., Buma, A. G., Nolting, R., Cadée, G., Jacques, G., and Treguer, P. (1990). On iron limitation of the southern ocean: experimental observations in the weddell and scotia seas. *Mar. Ecol. Prog. Ser.* 65, 105–122. doi: 10.3354/meps065105
- Demidov, A. B., Mosharov, S. A., and Gagarin, V. I. (2012). Meridional asymmetric distribution of the primary production in the Atlantic sector of the southern ocean in the austral spring and summer. *Oceanology* 52, 623–634. doi: 10.1134/S0001437012050050
- Deppeler, S. L., and Davidson, A. T. (2017). Southern ocean phytoplankton in a changing climate. *Front. Mar. Sci.* 4. doi: 10.3389/fmars.2017.00040
- DeVries, T., and Weber, T. (2017). The export and fate of organic matter in the ocean: New constraints from combining satellite and oceanographic tracer observations. *Global Biogeochem. Cycles* 31, 535–555. doi: 10.1002/2016GB005551
- Durack, P. J., and Wijffels, S. E. (2010). Fifty-year trends in global ocean salinities and their relationship to broad-scale warming. *J. Clim.* 23, 4342–4362. doi: 10.1175/2010JCLI3377.1
- Egan, L. (2008). *QuickChem method 31-107-04-1-C – nitrate and/or nitrite in brackish or seawater* (Colorado, USA: Lachat Instruments).
- Falkowski, P. G. (1997). Evolution of the nitrogen cycle and its influence on the biological sequestration of CO₂ in the ocean. *Nature* 387, 272–275. doi: 10.1038/387272a0
- Feng, Y., Hare, C. E., Leblanc, K., Rose, J. M., Zhang, Y., DiTullio, G. R., et al. (2009). Effects of increased pCO₂ and temperature on the north Atlantic spring bloom. i. the phytoplankton community and biogeochemical response. *Mar. Ecol. Prog. Ser.* 388, 13–25. doi: 10.3354/meps08133
- Finkel, Z. V., Beardall, J., Flynn, K. J., Quigg, A., Rees, T. A. V., and Raven, J. A. (2010). Phytoplankton in a changing world: cell size and elemental stoichiometry. *J. Plankton Res.* 32, 119–137. doi: 10.1093/plankt/fbp098
- GEOTRACES Intermediate Data Product Group (2021). *The GEOTRACES intermediate data product 2021 (IDP2021)*. (United Kingdom: NERC EDS British Oceanographic Data Centre NOC). doi: 10.5285/cf2d9ba9-d51d-3b7c-e053-8486abc0f5fd
- Gibberd, M. J., Kean, E., Barlow, R., Thomalla, S., and Lucas, M. (2013). Phytoplankton chemotaxonomy in the Atlantic sector of the southern ocean during late summer 2009. *Deep. Res. Part I Oceanogr. Res. Pap.* 78, 70–78. doi: 10.1016/j.dsr.2013.04.007
- Gorbanov, M., and Falkowski, P. (2004). “Fluorescence induction and relaxation (FIRE) technique and instrumentation for monitoring photosynthetic processes and primary production in aquatic ecosystems,” in *13th international congress of photosynthesis* (Montreal, QC: Allen Press), 1029–1031.
- Grasshoff, K., Ehrhardt, M., and Kremling, K. (1983). *Methods of seawater analysis. 2nd ed* (Verlag Chemie, Weinheim, New York) 14 (1), 419.
- Hardman-Mountford, N. J., Polimene, L., Hirata, T., Brewin, R. J., and Aiken, J. (2013). Impacts of light shading and nutrient enrichment geo-engineering approaches on the productivity of a stratified, oligotrophic ocean ecosystem. *J. R. Soc. Interface* 10 (89), 20130701. doi: 10.1098/rsif.2013.0701
- Harris, J. (2006). Antarctic marine protists? *2005th ed* in *Arctic, Antarctic, And alpine research*. Eds. FJ Scott and HJ Marchant. Canberra: Australian biological resources Study/Australian Antarctic division. 563 pp. doi: 10.1657/1523-0430(2006)38[301b:br]2.0.co;2
- Hauck, J., Völker, C., Wolf-Gladrow, D. A., Laufkötter, C., Vogt, M., Aumont, O., et al. (2015). On the southern ocean CO₂ uptake and the role of the biological carbon pump in the 21st century. *Global Biogeochem. Cycles* 29, 1451–1470. doi: 10.1002/2015GB005140
- Heiden, J. P., Völker, C., Jones, E. M., van de Poll, W. H., Buma, A. G., Meredith, M. P., et al. (2019). Impact of ocean acidification and high solar radiation on productivity and species composition of a late summer phytoplankton community of the coastal Western Antarctic peninsula. *Limnol. Oceanogr.* 64, 1716–1736. doi: 10.1002/lno.11147
- Henson, S. A., Sarmiento, J. L., Dunne, J. P., Bopp, L., Lima, I., Doney, S. C., et al. (2010). Detection of anthropogenic climate change in satellite records of ocean chlorophyll and productivity. *Biogeosciences* 7, 621–640. doi: 10.5194/bg-7-621-2010
- Hughes, D. J., Douglas, A., Campbell, M. A., Doblin, J. C., Kromkamp, E., Lawrenz, C., et al. (2018). Roadmaps and detours: Active chlorophyll- a assessments of primary productivity across marine and freshwater systems. *Environ. Sci. Technol.* 52, 12039–12054. doi: 10.1021/acs.est.8b03488
- Hutchins, D. A., and Boyd, P. W. (2016). Marine phytoplankton and the changing ocean iron cycle. *Nat. Clim. Change* 6, 1072–1079. doi: 10.1038/nclimate3147
- Hutchins, D. A., Sedwick, P. N., DiTullio, G. R., Boyd, P. W., Queguiner, B., Griffiths, F. B., et al. (2001). Control of phytoplankton growth by iron and silicic acid availability in the subantarctic southern ocean: Experimental results from the SAZ project. *J. Geophys. Res. Ocean.* 106, 31559–31572. doi: 10.1029/2000JC000333
- Juneau, P., and Harrison, P. J. (2005). Comparison by PAM fluorometry of photosynthetic activity of nine marine phytoplankton grown under identical conditions. *Photochem. Photobiol.* 81, 649–653. doi: 10.1562/2005-01-13-RA-414.1
- Koch, F., Beszteri, S., Harms, L., and Trimborn, S. (2019). The impacts of iron limitation and ocean acidification on the cellular stoichiometry, photophysiology, and transcriptome of phaeocystis antarctica. *Limnol. Oceanogr.* 64, 357–375. doi: 10.1002/lno.11045
- Kolber, Z. S., and Falkowski, P. G. (1992). “Fast repetition rate (FRR) fluorometer for making *In situ* measurements of primary productivity,” in *OCEANS 92 Proceedings in Mastering the Oceans Through Technology*. (Brookhaven National Lab., Upton, NY (United States: IEEE). 637–641. doi: 10.1109/OCEANS.1992.607657
- Kolber, Z. S., Prášil, O., and Falkowski, P. G. (1998). Measurements of variable chlorophyll fluorescence using fast repetition rate techniques: defining methodology and experimental protocols. *Biochim. Biophys. Acta - Bioenerg.* 1367, 88–106. doi: 10.1016/S0005-2728(98)00135-2
- Le Quéré, C., Takahashi, T., Buitenhuis, E. T., Rödenbeck, C., and Sutherland, S. C. (2010). Impact of climate change and variability on the global oceanic sink of CO₂. *Global Biogeochemical Cycles* 24 (4), GB4007. doi: 10.1029/2009GB003599
- Mackey, M. D., Mackey, D. J., Higgins, H. W., and Wright, S. W. (1996). CHEMTAX - a program for estimating class abundances from chemical markers: Application to HPLC measurements of phytoplankton. *Mar. Ecol. Prog. Ser.* 144, 265–283. doi: 10.3354/meps144265
- Mahadevan, A., D’asaro, E., Lee, C., and Perry, M. J. (2012). Eddy-driven stratification initiates north Atlantic spring phytoplankton blooms. *Science* 337, 54–58. doi: 10.1126/science.1218740
- Marañón, E., Lorenzo, M. P., Cermeño, P., and Mouriño-Carballido, B. (2018). Nutrient limitation suppresses the temperature dependence of phytoplankton metabolic rates. *ISME J.* 12, 1836–1845. doi: 10.1038/s41396-018-0105-1
- Marshall, A. G., Hemer, M. A., Hendon, H. H., and McInnes, K. L. (2018). Southern annular mode impacts on global ocean surface waves. *Ocean Model.* 129, 58–74. doi: 10.1016/j.ocemod.2018.07.007
- Matebr, R. J., and Hirst, A. C. (1999). Climate change feedback on the future oceanic CO₂ uptake. *Tellus B* 51, 722–733. doi: 10.1034/j.1600-0889.1999.t01-1-00012.x
- Maxwell, K., and Johnson, G. N. (2000). Chlorophyll fluorescence - a practical guide. *J. Exp. Bot.* 51, 659–668. doi: 10.1093/jxb/51.345.659
- Moore, C. M., Mills, M. M., Arrigo, K. R., Berman-Frank, I., Bopp, L., Boyd, P. W., et al. (2013). Processes and patterns of oceanic nutrient limitation. *Nat. Geosci.* 6, 701–710. doi: 10.1038/ngeo1765
- Moore, C. M., Seeyave, S., Hickman, A. E., Allen, J. T., Lucas, M. I., Planquette, H., et al. (2007). Iron-light interactions during the CROZEX natural iron bloom and EXPORT experiment (CROZEX) I: Phytoplankton growth and photophysiology. *Deep. Res. Part II Top. Stud. Oceanogr.* 54, 2045–2065. doi: 10.1016/j.dsr.2.2007.06.011
- Morel, F. M. M., and Price, N. M. (2003). The biogeochemical cycles of trace metals in the oceans. *Science* 300, 944–947. doi: 10.1126/science.1083545
- Mtshali, T. N., van Horsten, N. R., Thomalla, S. J., Ryan-Keogh, T. J., Nicholson, S. A., Roychoudhury, et al. (2019). Seasonal depletion of the dissolved iron reservoirs in the Sub-Antarctic zone of the southern Atlantic ocean. *Geophys. Res. Lett.* 46, 4386–4395. doi: 10.1029/2018GL081355
- Nunn, B. L., Faux, J. F., Hippmann, A. A., Maldonado, M. T., Harvey, H. R., Goodlett, D. R., et al. (2013). Diatom proteomics reveals unique acclimation strategies to mitigate fe limitation. *PLoS One* 8 (10), e75653. doi: 10.1371/journal.pone.0075653
- Orsi, A. H., Whitworth, T. III, and Nowlin, W. D. Jr. (1995). On the meridional extent and fronts of the Antarctic circumpolar current. *Deep Sea Res. Part I Oceanogr. Res. Pap.* 42, 641–673. doi: 10.1016/0967-0637(95)00021-W

- Owens, T. G., Falkowski, P. G., and Whitedge, T. E. (1980). Diel periodicity in cellular chlorophyll content in marine diatoms. *Mar. Biol.* 59, 71–77. doi: 10.1007/BF00405456
- Parsons, T., Maita, Y., and Lalli, C. (1984). *A manual of chemical and biological methods for seawater analysis* (Oxford: Pergamon).
- Petrou, K., Kranz, S. A., Trimborn, S., Hassler, C. S., Ameijeiras, S. B., Sackett, O., et al. (2016). Southern ocean phytoplankton physiology in a changing climate. *J. Plant Physiol.* 203, 135–150. doi: 10.1016/j.jplph.2016.05.004
- Pollard, R. T., Lucas, M. I., and Read, J. F. (2002). Physical controls on biogeochemical zonation in the southern ocean. *Deep Sea Res. Part II Top. Stud. Oceanogr.* 49, 3289–3305. doi: 10.1016/S0967-0645(02)00084-X
- Polvani, L. M., Waugh, D. W., Correa, G. J., and Son, S. W. (2011). Stratospheric ozone depletion: The main driver of twentieth-century atmospheric circulation changes in the southern hemisphere. *J. Clim.* 24, 795–812. doi: 10.1175/2010JCLI3772.1
- Raschka, S. (2018). MLxtend: Providing machine learning and data science utilities and extensions to python's scientific computing stack. *J. Open Source Softw.* 3 (24), 638. doi: 10.21105/joss.00638
- Ras, J., Claustre, H., and Uitz, J. (2008). Spatial variability of phytoplankton pigment distributions in the subtropical south pacific ocean: comparison between *in situ* and predicted data. *Biogeosciences* 5, 353–369. doi: 10.5194/bg-5-3409-2007
- Raven, J. A., Evans, M. C. W., and Korb, R. E. (1999). The role of trace metals in photosynthetic electron transport in O-2-evolving organisms. *Photosynth. Res.* 60, 111–149. doi: 10.1023/a:1006282714942
- Rio, M. H., Guinehut, S., and Larnicol, G. (2011). New CNES-CLS09 global mean dynamic topography computed from the combination of GRACE data, altimetry, and *in situ* measurements. *J. Geophys. Res. Ocean.* 116 (C7). doi: 10.1029/2010JC006505
- Ryan-Keogh, T., and Robinson, C. (2021). Phytoplankton photophysiology utilities: A Python toolbox for the standardization of processing active chlorophyll-a fluorescence data. *Front. Mar. Sci. Aquat. Physiol.* 8. doi: 10.3389/fmars.2021.525414
- Ryan-Keogh, T. J., Thomalla, S. J., Mtshali, T. N., and Little, H. (2017). Modelled estimates of spatial variability of iron stress in the Atlantic sector of the southern ocean. *Biogeosciences* 14, 3883–3897. doi: 10.5194/bg-14-3883-2017
- Ryan-Keogh, T. J., Thomalla, S. J., Mtshali, T. N., Van Horsten, N. R., and Little, H. J. (2018). Seasonal development of iron limitation in the sub-Antarctic zone. *Biogeosciences* 15, 4647–4660. doi: 10.5194/bg-15-4647-2018
- Sallée, J. B., Pellichero, V., Akhouldas, C., Pauthenet, E., Vignes, L., Schmidtko, S., et al. (2021). Summertime increases in upper-ocean stratification and mixed-layer depth. *Nature* 591, 592–598. doi: 10.1038/s41586-021-03303-x
- Schoffman, H., Lis, H., Shaked, Y., and Keren, N. (2016). Iron–Nutrient Interactions within Phytoplankton. *Front. Plant Sci.* 7, 1223. doi: 10.3389/fpls.2016.01223
- Sedwick, P., Blain, S., Quéguiner, B., Griffiths, F., Fiala, M., Bucciarelli, E., et al. (2002). Resource limitation of phytoplankton growth in the crozet basin, subantarctic southern ocean. *Deep Sea Res. Part II: Topical Stud. Oceanogr.* 49 (16), 3327–3349. doi: 10.1016/S0967-0645(02)00086-3
- Shen, A., Ma, Z., Jiang, K., and Li, D. (2016). Effects of temperature on growth, photophysiology, rubisco gene expression in *prorocentrum donghaiense* and *karenia mikimotoi*. *Ocean Sci. J.* 51, 581–589. doi: 10.1007/s12601-016-0056-2
- Sosik, H. M., and Olson, R. J. (2002). Phytoplankton and iron limitation of photosynthetic efficiency in the southern ocean during late summer. *Deep Sea Res. Part I Oceanogr. Res. Pap.* 49, 1195–1216. doi: 10.1016/S0967-0637(02)00015-8
- Sow, S., Trull, T., and Bodrossy, L. (2020). Oceanographic fronts shape phaeocystis assemblages: A high-resolution 18S rRNA gene survey from the ice-edge to the equator of the south pacific. *Front. Microbiol.* 11, 1847. doi: 10.3389/fmicb.2020.01847
- Spackeen, J. L., Bronk, D. A., Sipler, R. E., Bertrand, E. M., Hutchins, D. A., and Allen, A. E. (2018). Stoichiometric N:P ratios, temperature, and iron impact carbon and nitrogen uptake by Ross Sea microbial communities. *J. Geophys. Res. Biogeosci.* 123, 2955–2975. doi: 10.1029/2017JG004316
- Strzepek, R. F., Boyd, P. W., and Sunda, W. G. (2019). Photosynthetic adaptation to low iron, light, and temperature in southern ocean phytoplankton. *Proc. Natl. Acad. Sci.* 116, 4388–4393. doi: 10.1073/pnas.1810886116
- Strzepek, R. F., Hunter, K. A., Frew, R. D., Harrison, P. J., and Boyd, P. W. (2012). Iron-light interactions differ in southern ocean phytoplankton. *Limnol. Oceanogr.* 57, 1182–1200. doi: 10.4319/lo.2012.57.4.1182
- Suggett, D., Kraay, G., Holligan, P., Davey, M., Aiken, J., and Geider, R. (2001). Assessment of photosynthesis in a spring cyanobacterial bloom by use of a fast repetition rate fluorometer. *Limnol. Oceanogr.* 46, 802–810. doi: 10.4319/lo.2001.46.4.0802
- Suggett, D. J., Moore, C. M., Hickman, A. E., and Geider, R. J. (2009). Interpretation of fast repetition rate (FRR) fluorescence: Signatures of phytoplankton community structure versus physiological state. *Mar. Ecol. Prog. Ser.* 376, 1–19. doi: 10.3354/meps07830
- Suggett, D. J., Moore, C. M., Marañón, E., Omachi, C., Varela, R. A., Aiken, J., et al. (2006). Photosynthetic electron turnover in the tropical and subtropical Atlantic ocean. *Deep. Res. Part II Top. Stud. Oceanogr.* 53, 1573–1592. doi: 10.1016/j.dsr2.2006.05.014
- Sunda, W. G., and Huntsman, S. A. (1995). Iron uptake and growth limitation in oceanic and coastal phytoplankton. *Mar. Chem.* 50, 189–206. doi: 10.1016/0304-4203(95)00035-P
- Sunda, W. G., and Huntsman, S. A. (1997). Interrelated influence of iron, light and cell size on marine phytoplankton growth. *Nature* 390, 389–392. doi: 10.1038/37093
- Swart, N. C., Fyfe, J. C., Saenko, O. A., and Eby, M. (2014). Wind-driven changes in the ocean carbon sink. *Biogeosciences* 11, 6107–6117. doi: 10.5194/bg-11-6107-2014
- Swart, S., Thomalla, S., Monteiro, P., and Ansong, I. (2012). Mesoscale features and phytoplankton biomass at the GoodHope line in the southern ocean during austral summer. *Afr. J. Mar. Sci.* 34, 511–524. doi: 10.2989/1814232X.2012.749811
- Tagliabue, A., Sallée, J. B., Bowie, A. R., Lévy, M., Swart, S., and Boyd, P. W. (2014). Surface-water iron supplies in the southern ocean sustained by deep winter mixing. *Nat. Geosci.* 7, 314–320. doi: 10.1038/ngeo2101
- Takahashi, T., Sutherland, S. C., Sweeney, C., Poisson, A., Metz, N., Tilbrook, B., et al. (2002). Global sea-air CO₂ flux based on climatological surface ocean pCO₂, and seasonal biological and temperature effects. *Deep Sea Res. Part II Top. Stud. Oceanogr.* 49, 1601–1622. doi: 10.1016/S0967-0645(02)00003-6
- Thomalla, S. J., Fauchereau, N., Swart, S., and Monteiro, P. M. (2011). Regional scale characteristics of the seasonal cycle of chlorophyll in the southern ocean. *Biogeosciences* 8, 2849–2866. doi: 10.5194/bg-8-2849-2011
- Thomalla, S., Kean, E., Lucas, M., Gibberd, M. J., and Barlow, R. (2017). Photosynthesis versus irradiance relationships in the Atlantic sector of the southern ocean. *Afr. J. Mar. Sci.* 39, 43–57. doi: 10.2989/1814232X.2017.1303399
- Timmermans, K., Stolte, W., and de Baar, H. (1994). Iron-mediated effects on nitrate reductase in marine phytoplankton. *Mar. Biol.* 121 (2), 389–396. doi: 10.1007/BF00346749
- Timmermans, K. R., van der Woerd, H. J., Wernand, M. R., Sligting, M., Uitz, J., and de Baar, H. J. (2008). In situ and remote-sensed chlorophyll fluorescence as indicator of the physiological state of phytoplankton near the isles kerguelen (Southern ocean). *Polar Biol.* 31 (5), 617–628. doi: 10.1007/s00300-007-0398-4
- Uitz, J., Claustre, H., Morel, A., and Hooker, S. B. (2006). Vertical distribution of phytoplankton communities in open ocean: An assessment based on surface chlorophyll. *J. Geophys. Res. Ocean.* 111 (C8). doi: 10.1029/2005JC003207
- Vidussi, F., Claustre, H., Manca, B. B., Luchetta, A., and Jean-Claude, M. (2001). Phytoplankton pigment distribution in relation to upper Francesca claustre for the whole tchl a concentration mg estimated production value being mg m and the highest picophytoplankton contribution of tchl a gyres by low tchl a concentrations. *J. Geophys. Res.* 106, 939–956. doi: 10.1038/nm0497-414
- Viljoen, J. J., Philibert, R., Van Horsten, N., Mtshali, T., Roychoudhury, A. N., Thomalla, S., et al. (2018). Phytoplankton response in growth, photophysiology and community structure to iron and light in the polar frontal zone and Antarctic waters. *Deep Sea Res. Part I Oceanogr. Res. Pap.* 141, 118–129. doi: 10.2495/EEIA100071
- Welschmeyer, N. A. (1994). Fluorometric analysis of chlorophyll a in the presence of chlorophyll b and pheopigments. *Limnol. Oceanogr.* 39, 1985–1992. doi: 10.4319/lo.1994.39.8.1985
- Wolters, M. (2002). *Quickchem method 31-114-27-1-D – silicate in brackish or seawater* (Colorado, USA: Lachat Instruments).
- Wright, S. W., van den Enden, R. L., Pearce, I., Davidson, A. T., Scott, F. J., and Westwood, K. J. (2010). Phytoplankton community structure and stocks in the southern ocean (30–80° e) determined by CHEMTAX analysis of HPLC pigment signatures. *Deep Sea Res. Part II Top. Stud. Oceanogr.* 57, 758–778. doi: 10.1016/j.dsr2.2009.06.015